Available online at www.sciencedirect.com
ScienceDirect
Journal of Molecular Graphics and Modelling 26 (2007) 179–186
Journal of Molecular Graphics and Modelling
www.elsevier.com/locate/JMGM

Decomposition of nitrous oxide on carbon nanotubes

Supawadee Namuangruk [a,b], Pipat Khongpracha [a,b], Yuthana Tantirungrotechai [c], Jumras Limtrakul [a,b,*]

[a] *Laboratory for Computational and Applied Chemistry, Chemistry Department, Faculty of Science, Kasetsart University, Bangkok 10900, Thailand*
[b] *Center of Nanotechnology, Kasetsart University Research and Development Institute, Bangkok 10900, Thailand*
[c] *Department of Chemistry, Faculty of Science, Mahidol University, Rama 6 Road, Bangkok 10400, Thailand*

Received 11 May 2006; received in revised form 4 November 2006; accepted 8 November 2006
Available online 18 November 2006

Abstract

In this work, we have suggested the possibility of using carbon nanotubes to remove toxic gas. By taking an advantage of the density functional theory, we have investigated the decomposition of nitrous oxide (N_2O) on the sidewalls of the perfect and the Stone–Wales defect armchair (5,5)-SWNTs at the B3LYP/6-31G(d) level of theory. There are two reaction mechanisms proposed: stepwise and concerted pathways. Our calculations predict that the former route is kinetically favored on both the perfect and defect SWNTs with barrier heights of the rate-determining steps of 37.23 and 34.38 kcal/mol for the perfect and the defect systems, respectively. In the second pathway, the decomposition of nitrous oxide gas takes place in a single step with higher reaction barriers of 48.60 and 40.27 kcal/mol on the sidewalls of the perfect and the defect SWNTs, respectively. Moreover, we also demonstrated that an encapsulation of electron rich species, such as chloride anion, inside the channel of the SWNT can boost up the reaction rate of the N_2O decomposition on the SWNT. The chloride ion supplies excess electrons to the SWNT for transferring to the N_2O molecule causing lower reaction barriers in the reaction pathways.

Keywords: Nitrous oxide; Decomposition; Cycloaddition; Carbon nanotubes; Encapsulation

1. Introduction

Nitrous oxide (N_2O) is a toxic pollutant gas in the atmosphere, which often occurs during the incomplete combustion of fossil fuel. The major sources of the N_2O gas emission are chemical processes related to the production and utilization of nitric acid as fluidized bed combustion. Their contribution is about 20% of the total exhausted N_2O gas [1]. Responsible members of the public and industrialists are committing themselves to reduce greenhouse gases by at least 5–8% by the year 2012 [2]. The development of efficient technology for controlling N_2O emission is therefore considered as one of the top priorities. Two technologies for the conversion of N_2O to N_2 worth mentioning are the selective catalytic reduction (SCR) and the more appealing catalytic decomposition. The former is proceeded over Cu/ZSM-5 and Fe/ZSM-5 catalysts [3–6] while the latter is carried out over different catalytic systems, for example metal supported on TiO_2 and on ZSM-5 zeolite. However, under practical reaction conditions, most catalysts exhibit low activity [1]. Moreover, the activity of the catalyst is also inhibited by the fuel gas stream (O_2, H_2O, etc.). With problems such as these, the removal of N_2O is definitely a challenging issue.

Carbon nanotubes, especially single-wall carbon nanotubes (SWNTs), have attracted much attention for their fascinating structural, mechanical, electrical, and electromechanical properties [7–9]. These nano-structural materials can be modified by functionalization on the open ends or on the sidewall with organic or inorganic compounds to develop many interesting alternative applications. Recently, there have been several theoretical and experimental investigations which modify the sidewall of SWNTs by undergoing the 1,3-dipolar cycloaddition [10–12], (2 + 1) cycloaddition [13–19], fluorination [20–22], Diels-Alder cycloaddition [23–26], ozonolysis [27–31], and hydroboration [32] in order to introduce new physical and chemical properties. The decomposition of N_2O

* Corresponding author at: Laboratory for Computational and Applied Chemistry, Chemistry Department, Faculty of Science, Kasetsart University, Bangkok 10900, Thailand. Tel.: +662 9428900x323; fax: +662 9428900x324.
E-mail address: jumras.l@ku.ac.th (J. Limtrakul).

1093-3263/$ – see front matter © 2006 Elsevier Inc. All rights reserved.
doi:10.1016/j.jmgm.2006.11.003

over SWNTs may be another way of functionalization as this process is not only producing an epoxy adduct of SWNTs for further utilizations, but also converting a toxic N_2O to a nontoxic N_2 molecule. Therefore, in the catalytic aspect, the SWNTs might be a novel and excellent choice of catalyst for the nitrous oxide decomposition due to their high surface area and large number of active sites. In this aspect, the epoxy adduct, which is considered as a deactivated complex, can be reactivated easily by photodesorption of the oxygen to clean the SWNTs [33–35]. Hence, the understanding of the decomposition of N_2O to a N_2 reaction mechanism over SWNTs is useful as the basis for other catalytic applications.

This is the first attempt to study this idea to see if there is any possibility to use nanotube for the removal of toxic gas. In this study, we used the armchair (5,5)-SWNTs as a catalyst for nitrous oxide decomposition and predicted their reaction mechanisms. The roles of the defect and the presence of a chloride anion inside armchair (5,5)-SWNTs are also taken into consideration. These results would assist the experimentalists in selecting an effective condition for further explorations.

2. Computational details

In this work, we studied the decomposition of nitrous oxide at the perfect and the Stone–Wales defective sites on the sidewall of armchair (5,5)-SWNTs where the latter site is formed by a rotation of the π-bond by 90 degrees with respect to the perfect one (see Fig. 1a and b) [36]. A finite length of the armchair (5,5)-SWNT containing 90 carbon atoms was carefully selected to be representative of the SWNTs. The dangling bonds at the end of the fragment tube are terminated by hydrogen atoms giving a $C_{90}H_{20}$ model. It can be seen that there are two types of nonequivalent C–C pair sites, the 1,2-pair site and the 2,3-pair site on the sidewall of carbon nanotubes. However, the 1,2-pair site was verified to have a higher reactivity than the 2,3-pair site [27,15,37] in chemical functionalizations of the SWNTs.

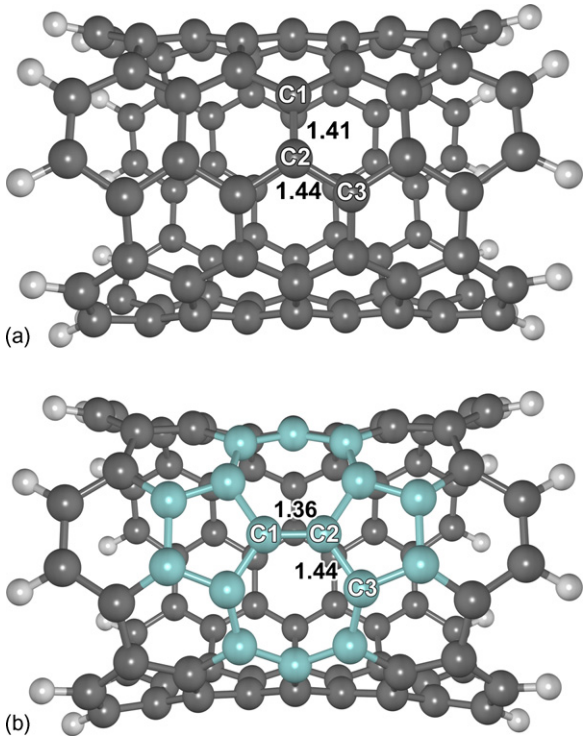

Fig. 1. Representation of the fragment tube of (a) perfect and (b) defective armchair (5,5)-SWNTs calculated at B3LYP/6-31G(d).

There are theoretical studies on the relationship of the chemical reactivities of the sidewall of (5,5) carbon nanotubes and the length of finite clusters [38,39]. From the nuclear-independent chemical shift (NICS) analysis and molecular orbital studies, Matsuo et al. [38] demonstrated that the chemical and electronic structures of carbon nanotubes oscillate as the tube is elongated from $C_{40}H_{20}$ to $C_{200}H_{20}$ generating Kekule', incomplete Clar and complete Clar networks in the periodicity of three. Without any indication of chemical modification, the author suggested that the complete Clar network in the series of $C_{60}H_{20}$, $C_{90}H_{20}$, $C_{120}H_{20}$, etc., having the smallest band gap should have the highest chemical reactivity. Afterward, Bettinger et al. [39], studied the carbene addition to the sidewall of the (5,5) armchair tube at the 1,2-pair site using finite clusters of various lengths. They concluded that the minimal model for studying the chemistry of the (5,5) armchair nanotubes should be the $C_{90}H_{20}$ model in which the effects from the edges in calculations are neglectable. Therefore, the data reported here were obtained from the $C_{90}H_{20}$ complete Clar network model at the 1,2-pair site. All calculations were carried out at the B3LYP level of theory with the 6-31G(d) basis set. Full optimizations and electronic population analysis of all stationary structures in the reaction pathways were carried out by the Gaussian 03 code [40].

3. Results and discussion

In this work, the B3LYP/6-31G(d) was performed to investigate the reaction mechanisms of the decomposition of the nitrous oxide molecule on the perfect (Section 3.1) and the Stone–Wales defective (Section 3.2) models. The effect of a chloride anion encapsulated in the SWNTs on the reactivity of both perfect and defective tubes is also discussed in Section 3.3.

3.1. Reaction mechanisms on the perfect (5,5) SWNT

For an asymmetric N_2O molecule, the N–O and N–N bond lengths are measured to be 1.192 and 1.135 Å, respectively, which are in good agreement with the experimental data of 1.184 and 1.128 Å, respectively. By comparison, the relevant theoretical to experimental studies [41,42], show evidence to prove that five-membered heterocycles can be formed in the cycloaddition of 1,3-dipole N_2O with double bonds in ethylene and surface diamond, implying that the double bond of carbon nanotubes could also form the five-membered ring with N_2O. In this work, we investigated the decomposition of nitrous oxide on the sidewall of SWNT by delivering the O atom in a N_2O molecule toward a C=C bond to form an epoxy adduct and a nitrogen molecule. The reaction mechanisms are proposed to

occur via the cyclic five-membered ring intermediate, called the stepwise mechanism (Subsection 3.3.1) or via directly losing the O atom denoted in the concerted mechanism (Subsection 3.3.2). The explanations of both mechanisms are clarified below.

3.1.1. Stepwise mechanism

The stepwise mechanism of the nitrous oxide decomposition on the sidewall of SWNT is characterized by the formation of the cyclic intermediate. The complexes related to this mechanism are shown in Fig. 2.

At the initial step, the N_2O molecule approaches the C1–C2 in a parallel direction, and the reaction subsequently proceeds via two consecutive steps. The first step is an asynchronous cycloaddition forming a cyclic intermediate (LM1p). At the transition state (TS1p), the cycloaddition occurs via an electron transfer from C1–C2 of the SWNT to the N_2O molecule causing a lengthening of C1–C2 from 1.41 to 1.49 Å. Moreover, alterations in the N_2O structure are observed. The angle of ∠ON2N1 is bent from 180° to 137.8° owing to a hybridization change from sp (linear) to nearly sp^2 (bent). It is also confirmed by a lengthening of bond distances, which compare with the

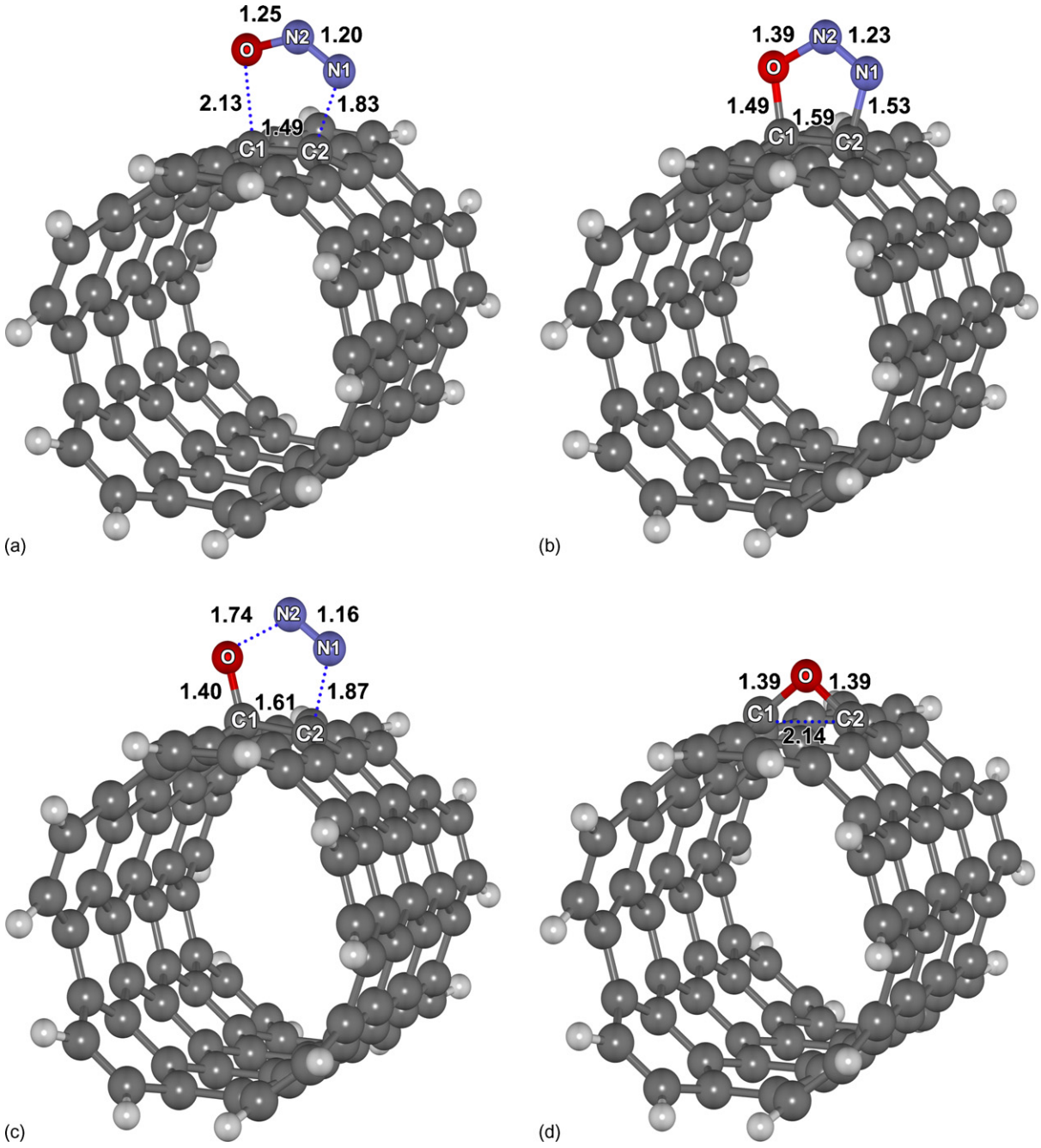

Fig. 2. The reaction complexes associated with the stepwise mechanism for the decomposition of nitrous oxide to nitrogen on the perfect site of the armchair (5,5)-SWNT. (a) TS1p (37.23), (b) LM1p (25.31), (c) TS2p (35.97), and (d) LM2p (−43.92). The values in parenthesis are the relative energies (in kcal/mol) of each individual complex with respect to the isolated molecules.

isolated N_2O molecule, by 0.06 Å for O–N2 and by 0.07 Å for N1–N2, which implies a weakening of those bonds in the N_2O molecule. Subsequently, after the cycloaddition process is completed, the metastable five-membered ring intermediate (LM1p) is formed with the adsorption energy of 25.31 kcal/mol. The hybridizations of atoms in the N_2O molecule are completely altered to sp^2. The O and N1 atoms are covalently bonded to C1 and C2 atoms with a single bond character (1.49 and 1.53 Å, respectively).

Lu et al. [27] studied the 1,3-dipolar cycloaddition of ozone (O_3) on an ONIOM2 model. Unlike a N_2O molecule, a symmetric O_3 molecule has a σ plane in between the left and right O-end atoms. Therefore, the reaction between O_3 and SWNT started from a synchronous cycloaddition with the σ_v symmetric transition state. The two forming C–O bonds are equivalent with a value of 2.29 Å.

For the second step, the cyclic intermediate expels a nitrogen molecule and forms an epoxy adduct. At this point, the reaction proceeds via the second transition state (TS2p) where the N1–N2 shortens (1.16 Å) to form the nitrogen molecule simultaneously with the lengthening of O–N2 and N1–C2 to 1.74 and 1.87 Å, respectively. At the final stage, the epoxy adduct is formed by complete expelling the nitrogen molecule.

All processes require the activation energy 37.23 kcal/mol relative to the isolated molecule. Fig. 6 clearly shows that the cycloaddition in the first step is the rate-determining step for nitrous oxide decomposition on the perfect nanotube. Since the heterocyclic intermediate is unstable, extrusion of the N2 molecule in the final step is more facile with a lower barrier of 10.66 kcal/mol with respect to the heterocyclic intermediate.

3.1.2. Concerted mechanism

Alternatively, the nitrous oxide decomposition on the sidewall of the perfect SWNT can proceed in a single step without forming the cyclic intermediate. This is called the concerted mechanism and its associated complexes are shown in Fig. 3.

In the concerted mechanism, the reaction proceeds when an O atom approaches the C1–C2 bond and transfers an O atom to the tube creating the epoxy adduct. At the transition state (TSp), the O atom is pointing to the C1–C2 bond with nonequivalent O···C1 and O···C2 bond distances of 2.31 and 1.77 Å, respectively. In comparison to the isolated N_2O molecule, the O–N2 lengthens from 1.19 to 1.47 Å and N1–N2 shortens from 1.13 to 1.14 Å. The O–N2–N1 is changed from a linear to a bent alignment on account of the changing of the electronic hybridization of the central atom in the N_2O molecule. Finally, the product is also in the form of an epoxy adduct that is equivalent to that in the stepwise mechanism.

The calculated activation barrier for the concerted mechanism is 48.60 kcal/mol. In comparison with the stepwise mechanism, this concerted mechanism is relatively kinetically unfavorable. Therefore, we can conclude that the stepwise mechanism is dominant and that the nitrous oxide favors to be decomposed on the sidewall of the perfect (5,5)-SWNT via the stepwise mechanism.

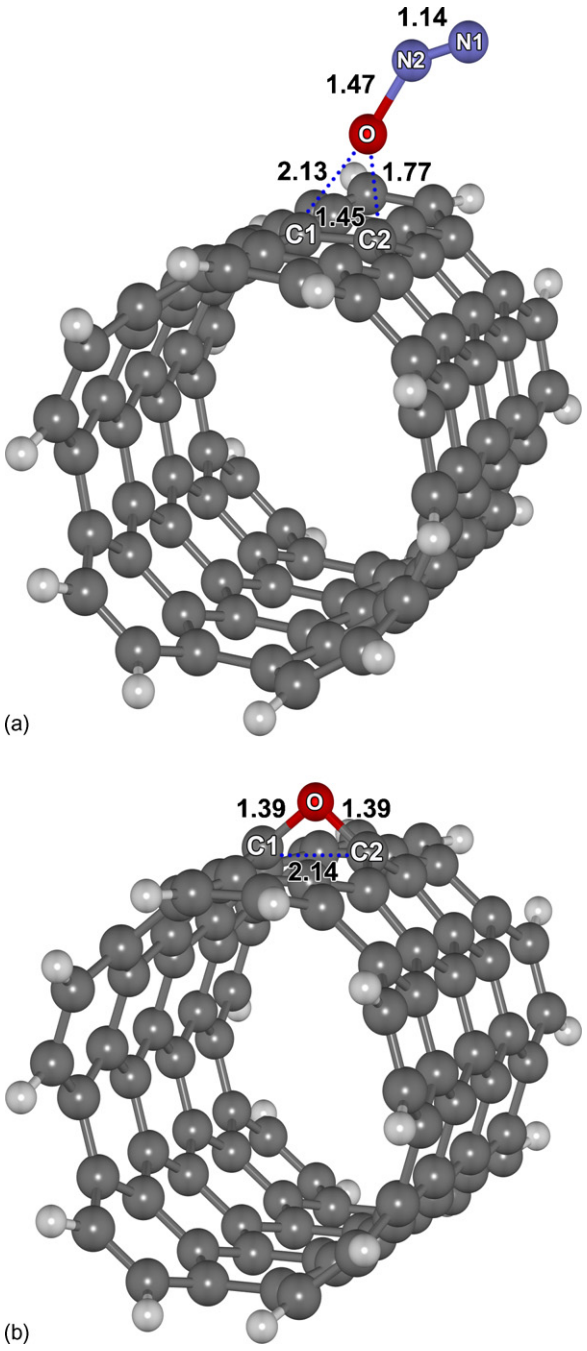

Fig. 3. The reaction complexes associated with the concerted mechanism for the decomposition of nitrous oxide to nitrogen on the perfect site of the armchair (5,5)-SWNT. (a) TSp (48.60), and (b) LM2p (−43.92). The values in parenthesis are the relative energies (in kcal/mol) of each individual complex with respect to the isolated molecules.

3.2. Reaction mechanisms on the Stone–Wales defect (5,5) SWNT

It is generally accepted that it is difficult to synthesize perfect nanotubes without defects, i.e. Stone–Wales defect, dopant, and vacancy [43]. In this section, we intend to examine the role of the Stone–Wales (SW) defect on the reaction pathway by focusing on a 7–7 ring fusion site which is the same

local bond center of the 1,2-pair site in the perfect model but it is rotated 90°. Even though the 7–7 ring fusion site is not the highest reactive site [36,44], it was considered to be the important reactive centers for chemical adsorptions [45,46] and reactions [24,46,47] on carbon nanotubes.

Figs. 4 and 5 show the optimized structure of all stationary points in the stepwise and concerted mechanisms for the decomposition of nitrous oxide at the 7–7 ring fusion of the Stone–Wales defect in (5,5)-SWNT (dSWNT). It is noted that the reaction mechanisms on the dSWNT are similar to those on the pSWNT (see Fig. 6). However, some energy crossings occurred which are due mainly to the instability of the epoxy product on the dSWNT. For the cycloaddition step, the activation barrier of the dSWNT model is lower than that of the pSWNT model by 2.85 kcal/mol. In other words, the cycloaddition of N_2O to the dSWNT is more facilitative than to the pSWNT model. To characterize these results, we consider the roles of N_2O and SWNT in the reaction. In the decomposition process, the N_2O molecule acts as the electron deficiency molecule while the SWNT acts as the electron donating part. Thus, electrons will be transferred from the SWNT to N_2O in order to undergo the decomposition process. From the fact that the shorter the bond is, the higher the electron in the local bond is. Hence, the higher electron density in the C1–C2 bond of the dSWNT should aid the cycloaddition reaction with incoming N_2O.

Contrary to the cycloaddition step, the barrier height for the second step involving the nitrogen molecule extrusion to form an epoxy adduct in the dSWNT system is higher than that in the pSWNT by 8.83 kcal/mol. This can be explained by the Bell–Evans–Polyani Principle: the more the exothermic reaction is the lower the barrier height. In this case, the epoxy adduct of the pSWNT, in which the oxygen atom is attached to the circumferential C1–C2 bond, can release the strain by opening the epoxy ring leaving the opened form (see Fig. 2d). For the dSWNT where the C1–C2 bond is in parallel with the tube, the epoxy ring forming via the axial addition is still in the closed form (see Fig. 4d). These cause different relative energies and the more stable epoxy adduct in the pSWNT by 13.36 kcal/mol. In addition to the reaction energy, we can observe the stabilities of the epoxy adducts in terms of the binding energies of triplet $O^{(t)}$ atoms attached to the sidewalls of those nanotubes. The calculated $O^{(t)}$ binding energies on the pSWNT and the dSWNT are −91.32 and −77.96 kcal/mol, respectively. Our observations

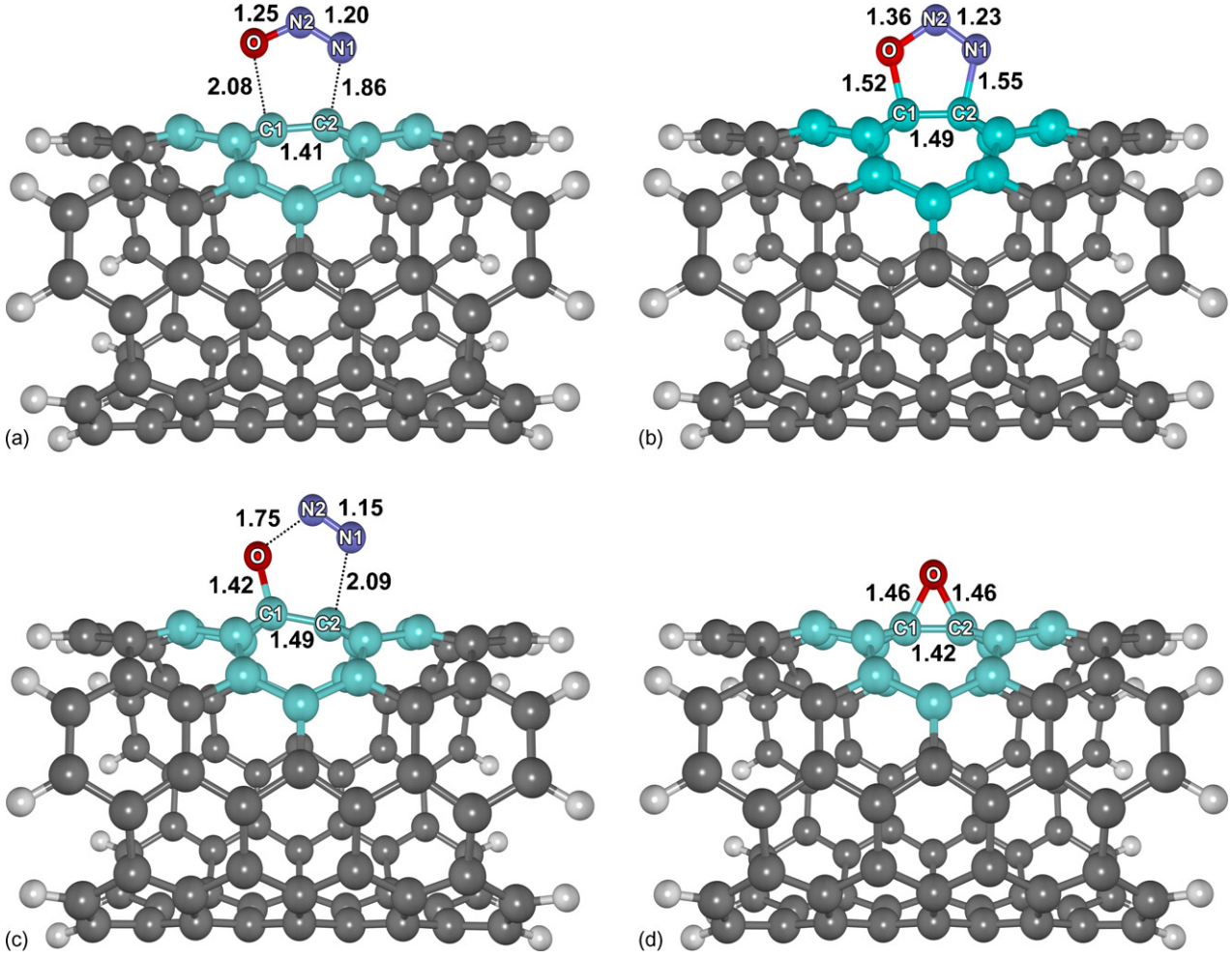

Fig. 4. The reaction complexes associated with the stepwise mechanism for the decomposition of nitrous oxide to nitrogen on the Stone–Wales defective site in the armchair (5,5)-SWNT. (a) TS1d (34.38), (b) LM1d (24.17), (c) TS2d (44.80), and (d) LM2d (−30.56). The values in parenthesis are the relative energies (in kcal/mol) of each individual complex with respect to the isolated molecules.

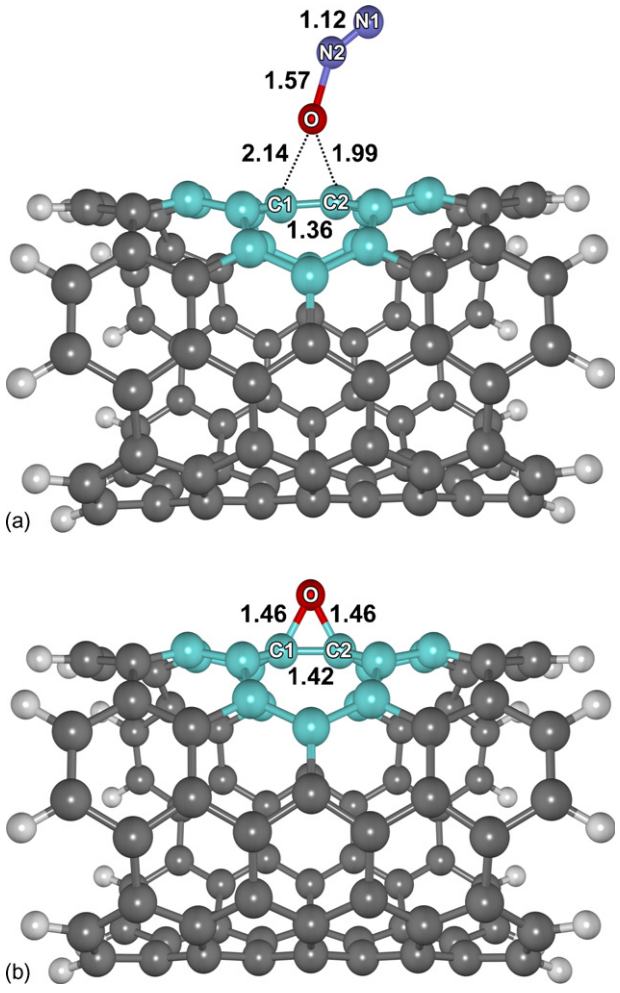

Fig. 5. The reaction complexes associated with the concerted mechanism for the decomposition of nitrous oxide to nitrogen on the Stone–Wales defective site in the armchair (5,5)-SWNT. (a) TSd (40.27), and (b) LM2d (−30.56). The values in parenthesis are the relative energies (in kcal/mol) of each individual complex with respect to the isolated molecules.

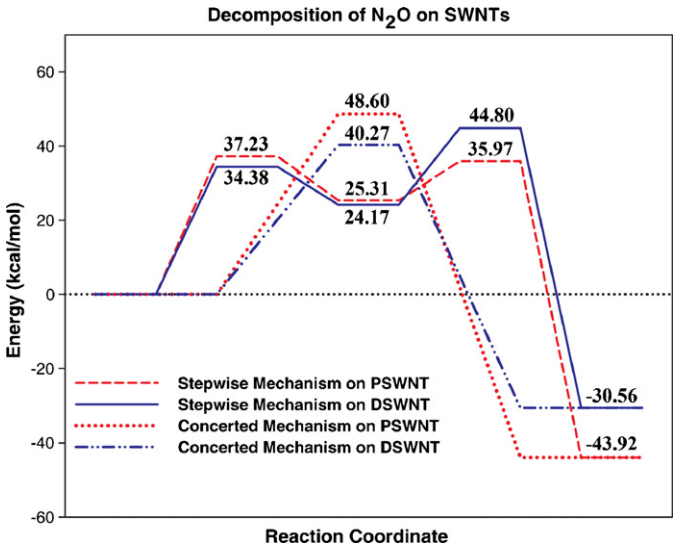

Fig. 6. Energy profiles for the nitrous oxide decomposition on pSWNT and dSWNT fully optimized at B3LYP/6-31G(d).

are in agreement with the Lu et al. work [44] that performed on the $C_{70}H_{20}$ model at the same level of theory. Their calculated additional energies are −74.6 and −62.4 kcal/mol for the pSWNT and the dSWNT systems, respectively. The differences in the values of their reaction energies and ours can be explained by the effect from edges in finite cluster calculations using their smaller model ($C_{70}H_{20}$). Moreover, based on Bettinger's and Matsuo's findings [38,39], the $C_{70}H_{20}$ tube model that possesses an incomplete Clar network is less reactive than the complete Clar network $C_{90}H_{20}$ model. However, in comparison to our results of 13.36 kcal/mol, this smaller model also estimates an energy difference of the two adducts by 12.2 kcal/mol on the potential energy surface.

3.3. Effect of Cl^-@SWNT on the reaction pathway

Since the activation energies of the decomposition of nitrous oxide on SWNT are rather high, in this section, a reduction of the barrier height of this reaction is studied. For the reason that the SWNT acts as a nucleophile, we expect that the introduction of an electron rich moiety into the SWNT might enhance its reactivity. As a case study, we doped the chloride anion into the SWNT (see Fig. 1) by encapsulating it in the middle tube of the SWNT (Cl^-@SWNT). The whole reaction process was completed by single point calculations at every stationary point at the same level of theory.

Using the explanation given in the Section 3.2, we indeed observe a certain relationship between a magnitude of electron gained on N_2O and the relative energy of the reaction complexes for the nitrous oxide decomposition (see Tables 1 and 2). The relationship states that the higher the electron gained on N_2O, the lower the relative energy at every point in

Table 1
The relative and activation barrier energies regarding the N_2O decomposition on the bare perfect and the defective SWNTs and the Chloride anion doped perfect and the defective SWNTs

SWNT	TS	TS1	LM1	TS2	LM2	$O^{(t)}$ addition	ΔE_a^1	ΔE_a^2
Bare								
Perfect	48.60	37.23	25.31	35.97	−43.92	−91.32, −74.6[a]	37.23	10.66
Defect	40.27	34.38	24.17	44.80	−30.56	−77.96, −62.4[a]	34.38	20.63
Cl^-@								
Perfect	44.50	32.21	20.94	31.21	−44.64	−92.03	32.21	10.27
Defect	38.34	32.13	23.82	41.76	−30.61	−78.00	32.13	17.93

[a] Lu et al. work [44].

Table 2
The charge gained on N_2O of all stationary points of N_2O decomposition on the bare perfect site (pSWNT), the defective site (dSWNT) and the Chloride anion doped perfect site (Cl^-@pSWNT), the defective site (Cl^-@dSWNT) of (5,5) SWNT

	pSWNT	Cl^-@pSWNT	dSWNT	Cl^-@dSWNT
Stepwise				
TS1	−0.2797	−0.3561	−0.2724	−0.3538
LM1	−0.4196	−0.4764	−0.4076	−0.4647
TS2	−0.5544	−0.6144	−0.5696	−0.6398
LM2	−0.5576	−0.5723	−0.4759	−0.5123
Concerted				
TS	−0.2611	−0.4432	−0.2934	−0.3926

the reaction pathway. The barrier heights are decreased in the following order: Bare pSWNT > Cl^-@pSWNT and Bare dSWNT > Cl^-@dSWNT. These findings suggest that introducing an excess electron density onto the (5,5) armchair carbon nanotube can improve the reaction kinetics for decomposition of nitrous oxide onto the sidewall of SWNTs by enlarging the magnitude of the electron transfer from SWNTs to the N_2O molecule. Besides the encapsulation of the anion, we also applied metal atom decorated side-walled nanotubes and fullerenes as catalytic models for N_2O decomposition reaction. We observed a rapid decomposition of N_2O on the Ti decorated side-walled nanotubes at room temperature. The results will be published elsewhere.

4. Conclusion

The decomposition of a nitrous oxide molecule on the sidewall of the perfect- and the Stone–Wales defect (5,5)-SWNTs have been studied from the first principle calculations. The predicted reaction mechanisms (the stepwise and concerted mechanisms) are analogous for the perfect and the defective models. For the stepwise mechanism, the reaction occurs through a cyclic intermediate via an asynchronous cycloaddition and followed by the extrusion of a nitrogen molecule. The activation barrier for the rate-determining cycloaddition step is calculated to be 37.23 kcal/mol for the perfect and 34.38 kcal/mol for the defective models, respectively. The five-membered ring complex is an unstable intermediate and results a low activation barrier in the final step (10.66 kcal/mol for the perfect and 20.63 kcal/mol for the defective models, respectively). For the concerted mechanism, the nitrous oxide molecule directly transfers an O atom to the SWNT in a single step. The activation barriers are evaluated to be 48.60 kcal/mol for the perfect and 40.27 kcal/mol for the defective models, respectively. The reaction barriers in the concerted mechanism are higher than those in the stepwise mechanism. Therefore, we concluded that the nitrous oxide molecule can be decomposed favorably on the armchair (5,5)-SWNT via the stepwise mechanism.

The effect of a chloride anion encapsulated into the SWNTs has also been studied. It is clearly demonstrated that the presence of the chloride anion inside the channel of the SWNTs increases the catalytic reactivity of the SWNTs for the nitrous oxide decomposition on the perfect and the Stone–Wales defect SWNTs by enhancing the electron transfer from the tube to the N_2O molecule. Although the calculated smallest barrier for these systems (34.38 kcal/mol) is rather high, we hope that this study would assist the experimentalists in fine-tuning an effective condition of further explorations which may lead to a new efficient process for the removal of toxic N_2O gas in the future.

Acknowledgements

This work was supported in part by grants from the Thailand Research Fund, TRF Senior Research Scholar to JL and the Royal Golden Jubilee Ph.D. Program to SN, and the Kasetsart University Research and Development Institute (KURDI), as well as the Ministry of University Affairs under the Science and Technology Higher Education Development Project (MUA-ADB funds). Support from the National Nanotechnology Center under the National Science and Technology Development Agency is also acknowledged.

References

[1] F. Kapteijn, J. Rodriguez-Mirasol, J.A. Moulijn, Heterogeneous catalytic decomposition of nitrous oxide, Appl. Catal. B 9 (1996) 25–64.
[2] S.C. Christoforou, E.A. Efthimiadis, I.A. Vasalos, Catalytic conversion of N_2O to N2 over metal-based catalysts in the presence of hydrocarbons and oxygen, Catal. Lett. 79 (2002) 137–147.
[3] K. Yamada, C. Pophal, K. Segawa, Selective catalytic reduction of N_2O by C3H6 over Fe–ZSM-5, Micropor. Mesopor. Mater. 21 (1998) 549–555.
[4] G. Centi, F. Vazzana, Selective catalytic reduction of N_2O in industrial emissions containing O_2, H_2O and SO_2: behavior of Fe/ZSM-5 catalysts, Catal. Today 53 (1999) 683–693.
[5] K. Yamada, S. Kondo, K. Segawa, Selective catalytic reduction of nitrous oxide over Fe–ZSM-5: the effect of ion-exchange level, Micropor. Mesopor. Mater. 35–36 (2000) 227–234.
[6] S. Pabchanda, P. Pantu, D. Tantanak, J. Limtrakul, Structure and energetics of nitrous oxide and methane adsorption on the Fe–ZSM-5 zeolite: ONIOM and density functional studies, Stud. Surf. Sci. Catal. 154B (2004) 1844–1848.
[7] C. Dekker, Carbon nanotubes as molecular quantum wires, Phys. Today 52 (1999) 22–28.
[8] P. Avouris, Molecular electronics with carbon nanotubes, Accounts Chem. Res. 35 (2002) 1026–1034.
[9] M. Ouyang, J.-L. Huang, C.M. Lieber, Fundamental electronic properties and applications of single-walled carbon nanotubes, Accounts Chem. Res. 35 (2002) 1018–1025.
[10] V. Georgakilas, K. Kordatos, M. Prato, D.M. Guldi, M. Holzinger, A. Hirsch, Organic functionalization of carbon nanotubes, J. Am. Chem. Soc. 124 (2002) 760–761.
[11] X. Lu, F. Tian, X. Xu, N. Wang, Q. Zhang, A theoretical exploration of the 1,3-dipolar cycloadditions onto the sidewalls of (*n*,*n*) armchair single-wall carbon nanotubes, J. Am. Chem. Soc. 125 (2003) 10459–10464.
[12] N. Tagmatarchis, M. Prato, Functionalization of carbon nanotubes via 1,3-dipolar cycloadditions, J. Mater. Chem. 14 (2004) 437–439.
[13] R. Li, Z. Shang, G. Wang, Y. Pan, Z. Cai, X. Zhao, Study on dichlorocarbene cycloaddition isomers of armchair single-walled carbon nanotubes, Theochem. J. Mol. Struct. 583 (2002) 241–247.
[14] H. Hu, B. Zhao, M.A. Hamon, K. Kamaras, M.E. Itkis, R.C. Haddon, Sidewall functionalization of single-walled carbon nanotubes by addition of dichlorocarbene, J. Am. Chem. Soc. 125 (2003) 14893–14900.
[15] X. Lu, F. Tian, Q. Zhang, The [2 + 1] cycloadditions of dichlorocarbene, silylene, germylene, and oxycarbonylnitrene onto the sidewall of armchair (5,5) single-wall carbon nanotube, J. Phys. Chem. B 107 (2003) 8388–8391.

[16] Y.-Y. Chu, M.-D. Su, Theoretical study of addition reactions of carbene, silylene, and germylene to carbon nanotubes, Chem. Phys. Lett. 394 (2004) 231–237.
[17] M. Holzinger, J. Steinmetz, D. Samaille, M. Glerup, M. Paillet, P. Bernier, L. Ley, R. Graupner, [2 + 1] cycloaddition for cross-linking SWCNTs, Carbon 42 (2004) 941–947.
[18] J. Lu, S. Nagase, X. Zhang, Y. Maeda, T. Wakahara, T. Nakahodo, T. Tsuchiya, T. Akasaka, D. Yu, Z. Gao, R. Han, H. Ye, Structural evolution of [2 + 1] cycloaddition derivatives of single-wall carbon nanotubes: from open structure to closed three-membered ring structure with increasing tube diameter, Theochem. J. Mol. Struct. 725 (2005) 255–257.
[19] M.-D. Su, Theoretical study of addition reactions of heavy carbenes to carbon and boron nitride nanotubes, J. Phys. Chem. B 109 (2005) 21647–21657.
[20] T. Nakajima, S. Kasamatsu, Y. Matsuo, Synthesis and characterization of fluorinated carbon nanotube, Eur. J. Solid State Inor. 33 (1996) 831–840.
[21] N.G. Lebedev, I.V. Zaporotskova, L.A. Chernozatonskii, Fluorination of carbon nanotubes: quantum chemical investigation within MNDO approximation, Int. J. Quant. Chem. 96 (2003) 142–148.
[22] S. Kawasaki, K. Komatsu, F. Okino, H. Touhara, H. Kataura, Fluorination of open- and closed-end single-walled carbon nanotubes, Phys. Chem. Chem. Phys. 6 (2004) 1769–1772.
[23] X. Lu, F. Tian, N. Wang, Q. Zhang, Organic functionalization of the sidewalls of carbon nanotubes by Diels–Alder reactions: a theoretical prediction, Org. Lett. 4 (2002) 4313–4315.
[24] J.L. Delgado, P. de la Cruz, F. Langa, A. Urbina, J. Casado, J.T. Lopez Navarrete, Microwave-assisted sidewall functionalization of single-wall carbon nanotubes by Diels–Alder cycloaddition, Chem. Commun. (2004) 1734–1735.
[25] C. Warakulwit, S. Bamrungsap, P. Luksirikul, P. Khongpracha, J. Limtrakul, Diels–Alder cycloadditions of single-wall carbon nanotubes with electron-rich dienes: a theoretical study, Stud. Surf. Sci. Catal. 156 (2005) 823–828.
[26] L. Zhang, J. Yang, L. Edwards Christopher, B. Alemany Lawrence, N. Khabashesku Valery, R. Barron Andrew, Diels–Alder addition to fluorinated single walled carbon nanotubes, Chem. Commun. (2005) 3265–3267.
[27] X. Lu, L. Zhang, X. Xu, N. Wang, Q. Zhang, Can the sidewalls of single-wall carbon nanotubes be ozonized? J. Phys. Chem. B 106 (2002) 2136–2139.
[28] S. Picozzi, S. Santucci, L. Lozzi, C. Cantalini, C. Baratto, G. Sberveglieri, I. Armentano, J.M. Kenny, L. Valentini, B. Delley, Ozone adsorption on carbon nanotubes: ab initio calculations and experiments, J. Vac. Sci. Technol. A 22 (2004) 1466–1470.
[29] S. Picozzi, S. Santucci, L. Lozzi, L. Valentini, B. Delley, Ozone adsorption on carbon nanotubes. The role of Stone–Wales defects, J. Chem. Phys. 120 (2004) 7147–7152.
[30] W.L. Yim, Z.F. Liu, A reexamination of the chemisorption and desorption of ozone on the exterior of a (5,5) single-walled carbon nanotube, Chem. Phys. Lett. 398 (2004) 297–303.
[31] L.V. Liu, W.Q. Tian, Y.A. Wang, Ozonization at the vacancy defect site of the single-walled carbon nanotube, J. Phys. Chem. B 110 (2006) 13037–13044.
[32] L. Long, X. Lu, F. Tian, Q. Zhang, Hydroboration of C(1 0 0) surface, fullerene, and the sidewalls of single-wall carbon nanotubes with borane, J. Org. Chem. 68 (2003) 4495–4498.
[33] L.G. Zhou, S.-Q. Shi, Formation energy of Stone–Wales defects in carbon nanotubes, Appl. Phys. Lett. 83 (2003) 1222–1224.
[34] Y. Miyamoto, N. Jinbo, H. Nakamura, A. Rubio, D. Tomanek, Photodesorption of oxygen from carbon nanotubes, Phys. Rev. B 70 (2004) 233401–233404.
[35] M. Shim, J.H. Back, T. Ozel, K.-W. Kwon, Effects of oxygen on the electron transport properties of carbon nanotubes. Ultraviolet desorption and thermally induced processes, Phys. Rev. B 71 (2005) 205411–205419.
[36] H.F. Bettinger, The reactivity of defects at the sidewalls of single-walled carbon nanotubes: the Stone–Wales defect, J. Phys. Chem. B 109 (2005) 6922–6924.
[37] H.F. Bettinger, Addition of carbenes to the sidewalls of single-walled carbon nanotubes, Chem. Eur. J. 12 (2006) 4372–4379.
[38] Y. Matsuo, K. Tahara, E. Nakamura, Theoretical studies on structures and aromaticity of finite-length armchair carbon nanotubes, Org. Lett. 5 (2003) 3181–3184.
[39] H.F. Bettinger, Effects of finite carbon nanotube length on sidewall addition of fluorine atom and methylene, Org. Lett. 6 (2004) 731–734.
[40] M.J. Frisch, G.W. Trucks, H.B. Schlegel, G.E. Scuseria, M.A. Robb, J.R. Cheeseman, J.A. Montgomery, Jr., T. Vreven, K.N. Kudin, J.C. Burant, J.M. Millam, S.S. Iyengar, J. Tomasi, V. Barone, B. Mennucci, M. Cossi, G. Scalmani, N. Rega, G.A. Petersson, H. Nakatsuji, M. Hada, M. Ehara, K. Toyota, R. Fukuda, J. Hasegawa, M. Ishida, T. Nakajima, Y. Honda, O. Kitao, H. Nakai, M. Klene, X. Li, J.E. Knox, H.P. Hratchian, J.B. Cross, C. Adamo, J. Jaramillo, R. Gomperts, R.E. Stratmann, O. Yazyev, A.J. Austin, R. Cammi, C. Pomelli, J.W. Ochterski, P.Y. Ayala, K. Morokuma, G.A. Voth, P. Salvador, J.J. Dannenberg, V.G. Zakrzewski, S. Dapprich, A.D. Daniels, M.C. Strain, O. Farkas, D.K. Malick, A.D. Rabuck, K. Raghavachari, J.B. Foresman, J.V. Ortiz, Q. Cui, A.G. Baboul, S. Clifford, J. Cioslowski, B.B. Stefanov, G. Liu, A. Liashenko, P. Piskorz, I. Komaromi, R.L. Martin, D.J. Fox, T. Keith, M.A. Al-Laham, C.Y. Peng, A. Nanayakkara, M. Challacombe, P.M.W. Gill, B. Johnson, W. Chen, M.W. Wong, C. Gonzalez, J.A. Pople, Gaussian 03, Revision B.05, Gaussian, Inc., Wallingford, CT, 2004.
[41] M.-D. Su, H.-Y. Liao, W.-S. Chung, S.-Y. Chu, Cycloadditions of 16-electron 1,3-dipoles with ethylene. A density functional and CCSD(T) study, J. Org. Chem. 64 (1999) 6710–6716.
[42] X. Lu, X. Xu, N. Wang, Q. Zhang, A DFT study of the 1,3-dipolar cycloadditions on the C(1 0 0)-2 × 1 surface, J. Org. Chem. 67 (2002) 515–520.
[43] J.C. Charlier, Defects in carbon nanotubes, Accounts Chem. Res. 35 (2002) 1063–1069.
[44] X. Lu, Z. Chen, P.V.R. Schleyer, Are Stone–Wales defect sites always more reactive than perfect sites in the sidewalls of single-wall carbon nanotubes? J. Am. Chem. Soc. 127 (2005) 20–21.
[45] N. Chakrapani, Y.M. Zhang, S.K. Nayak, J.A. Moore, D.L. Carroll, Y.Y. Choi, P.M. Ajayan, Chemisorption of acetone on carbon nanotubes, J. Phys. Chem. B 107 (2003) 9308–9311.
[46] C. Wang, G. Zhou, H. Liu, J. Wu, Y. Qiu, B.-L. Gu, W. Duan, Chemical functionalization of carbon nanotubes by carboxyl groups on Stone–Wales defects: a density functional theory study, J. Phys. Chem. B 110 (2006) 10266–10271.
[47] X. Wu, J. Yang, J.G. Hou, Q. Zhu, Defects-enhanced dissociation of H_2 on boron nitride nanotubes, J. Chem. Phys. 124 (2006) 054701–054705.